

Squeezed noise due to two-level system defects in superconducting resonator circuits

So Takei,¹ Victor M. Galitski,^{1,2} and Kevin D. Osborn³

¹Condensed Matter Theory Center, Department of Physics, The University of Maryland College Park, MD 20742

²Joint Quantum Institute, Department of Physics, The University of Maryland College Park, MD 20742

³Laboratory for Physical Sciences, College Park, MD 20740

(Dated: October 23, 2018)

Motivated by recent surprising experimental results for the noise output of superconducting microfabricated resonators used in quantum computing applications and astronomy, we develop a fully quantum theoretical model to describe quantum dynamics of these circuits. Building on theoretical techniques from quantum optics, we calculate the noise in the output voltage due to two-level system (TLS) defects. The theory predicts squeezing for the noise in the amplitude quadrature with respect to the input noise, which qualitatively reproduces the noise ellipse observed in experiment. We show that noise enhancement along the phase direction persists for pump frequencies away from resonance. Our results also suggest that intrinsic TLS fluctuations must be incorporated in the model in order to describe the experimentally observed dependence of the phase noise on input power.

PACS numbers: 03.67.-a, 03.65.Yz, 77.22.Gm, 85.25.-j

Amorphous dielectrics contain weakly-coupled two-level system (TLS) defects [1, 2] that are known to modify the complex permittivity at low temperatures, including the imaginary part which is responsible for loss [3]. In Josephson qubits the purposeful amorphous dielectrics were found to contain TLSs which leads to decoherence [4]. Similarly, the loss in superconducting resonators is generally attributed to TLS defects which can arise from the native oxides on the superconducting leads [5] or deposited amorphous dielectrics [6, 7]. Superconducting resonators are used in applications of quantum computing [8] and as single photon detectors for astronomy, where noise can limit the detection performance [9] and may be attributable to TLSs [10]. Surprisingly, recent studies have revealed that the amplitude noise quadrature of resonators is limited by the experimental sensitivity near the vacuum noise limit [11]. In contrast, noise in the phase quadrature is relatively large and decreases as the square root of the measurement power [12]. A semi-empirical model was used to describe this phase noise saturation, but a quantitative model of phase-amplitude noise asymmetry is still lacking [13].

Previous related noise studies have considered the effects of TLS noise on superconducting qubits [14], and noise squeezing in various nonlinear systems including Josephson junction parametric amplifiers [15, 16], micro-cantilevers [17], and nanomechanical resonators coupled to a Cooper-pair box [18]. Atoms have also been used for four-wave mixing experiments to squeeze optical cavity states [19].

In this letter, we develop a theory for noise due to TLS defects in a superconducting resonator circuit. We compute the noise in the transmitted voltage for the system shown in Fig. 1(a) assuming that the lone source of stochastic fluctuations are the quadrature-independent white noise in the incident voltages on the transmission lines. The theory predicts that squeezing in the transmitted noise generally occurs even if the dynamics of the internal resonator, including the TLSs, is fully deterministic. The results imply that intrinsic stochastic dynamics of TLSs is not necessary in explaining the observed squeezing in the transmitted voltage noise. Our work

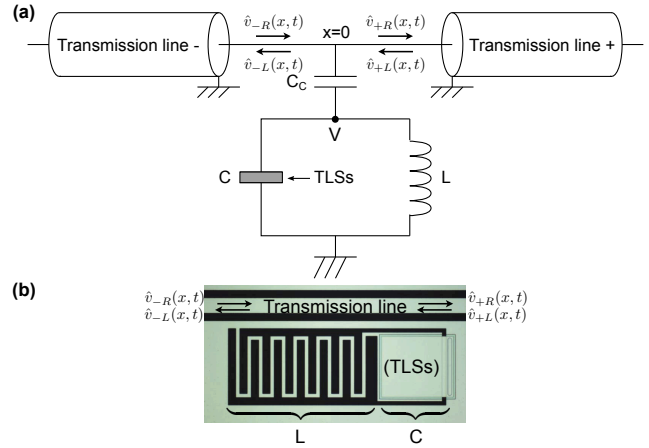


FIG. 1: (a) A circuit diagram of the considered setup. (b) Actual image (taken from Ref. 6) of a notch-type aluminum LC resonator which can be modelled using (a). The components are labelled to clarify its correspondence to circuit in (a).

shows a similarity between noise squeezing from TLS defects in these devices [11, 12] and squeezing of coherent light due to two-level atoms in quantum optics [20]. We also compute noise power for off-resonant pump frequencies and confirm that enhancement in the phase noise and squeezing in the amplitude noise persists away from resonance.

We have two identical semi-infinite 1D transmission lines, labeled $-$ and $+$, which are attached to each other end-to-end at $x = 0$ (see Fig. 1(a)). They are coupled to the internal superconducting LC resonator at $x = 0$ through the coupling capacitor C_c . The capacitor and inductor in the LC circuit have capacitance C and inductance L . Here, we take $C_c \ll C$, and consider the case where TLS defects reside only inside the dielectric of capacitor C . A microwave source (not shown) sends in a pump signal from $x = -\infty$, and we focus on the transmitted voltage noise on transmission line $+$.

The Hamiltonian for the full system has three terms, $\hat{H} = \hat{H}_0 + \hat{H}_{\text{TLS}} + \hat{H}_{\text{TLS-R}}$. $\hat{H}_0 = \sum_{m=\{+,-\}} \hat{H}_m + \hat{H}_R$ models the two

transmission lines and the internal resonator,

$$\hat{H}_m = \int dx \Theta(mx) \left[\frac{\hat{P}_m^2(x)}{2\ell} + \frac{(\nabla_x \hat{Q}_m(x))^2}{2c} \right] \quad (1)$$

$$\hat{H}_R = \frac{\hat{P}_L^2}{2L} + \frac{\hat{Q}_0^2}{2C_c} + \frac{(\hat{Q}_0 - \hat{Q}_L)^2}{2C}, \quad (2)$$

where $m = \{+, -\}$ labels the left ($-$) and right ($+$) transmission lines, and $\Theta(x)$ is the unit step function. $\hat{Q}_m(x)$ is the operator for total charge residing to the right of x on transmission line m , \hat{Q}_L is the operator for total charge that has flowed through the inductor, and $\hat{Q}_0 = (\hat{Q}_- - \hat{Q}_+)|_{x=0}$ denotes the total charge operator on capacitor C_c . \hat{P}_m and \hat{P}_L are the conjugate momenta for \hat{Q}_m and \hat{Q}_L , respectively, and they satisfy $[\hat{Q}_m(x), \hat{P}_{m'}(x')] = i\hbar \delta_{mm'} \delta(x - x')$ and $[\hat{Q}_L, \hat{P}_L] = i\hbar$, where $m, m' = \{+, -\}$. The transmission lines are modeled as conductors with inductance per unit length ℓ , capacitance to ground per unit length c , and characteristic impedance $Z = \sqrt{\ell/c}$ [21, 22]. We assume we have N identical and independent TLSs, all with asymmetry energy Δ_A and tunneling energy Δ_0 . The TLS Hamiltonian is then given by $\hat{H}_{\text{TLS}} = \Delta_A \hat{S}_z + \Delta_0 \hat{S}_x$, where $\hat{S}_i = \sum_{\alpha=1}^N \hat{s}_{i\alpha}$ is the collective spin operator which represents the N TLSs, and $\hat{s}_{i\alpha} = \sigma_i/2$ with the usual Pauli matrices σ_i . The components of the collective spin operator obey $[\hat{S}_i, \hat{S}_j] = i\epsilon_{ijk} \hat{S}_k$. After diagonalization $\hat{H}_{\text{TLS}} = E \hat{S}_z$ where $E = [\Delta_A^2 + \Delta_0^2]^{1/2}$. Each TLS interacts with the uniform electric field inside the capacitor through its electric dipole moment \mathbf{p} . We assume the dipoles fluctuate by making 180° flips between parallel and anti-parallel orientations with respect to the field. The field affects the asymmetry energy and here we ignore the relatively small changes to the tunnel barrier, similar to other treatments of TLSs derived from the tunneling model [1]. In the diagonalized basis the interaction between the TLSs and the field can then be written as $\hat{H}_{\text{TLS-R}} = g\hbar[\hat{S}_z \cot 2\xi + (\hat{S}^+ + \hat{S}^-)/2](\hat{Q}_0 - \hat{Q}_L)$, where the coupling constant $g = 2|\mathbf{p}| \sin 2\xi / \hbar C d$, d is the separation between the plates of the capacitor, ξ is defined via $\tan 2\xi = \Delta_0 / \Delta_A$, and $\hat{S}^\pm = \hat{S}_x \pm i\hat{S}_y$. We use $|\mathbf{p}| = 1$ Debye, which is comparable to the dipole moment sizes observed for TLSs in amorphous SiO_2 at microwave frequencies and OH rotors in AlO_x [23].

For $x \neq 0$, $\hat{Q}_m(x, t)$ obey the massless scalar Klein-Gordon equation, and the solution can be written as a sum of right- (R) and left-propagating (L) components, i.e. $\hat{Q}_m(x, t) = \hat{Q}_{mR}(x, t) + \hat{Q}_{mL}(x, t)$, where

$$\hat{Q}_{m\{R,L\}}(x, t) = \int_0^\infty \frac{d\omega}{2\pi} \sqrt{\frac{\Omega_r}{\omega}} \hat{q}_{m\{R,L\}}^\dagger(\omega) e^{i\omega(t \mp x/v)} + h.c., \quad (3)$$

$v = (\ell c)^{-1/2}$ is the velocity of wave propagation and Ω_r is the resonance frequency of the loaded LC circuit. The charge operators obey $[\hat{q}_{m\tau}(\omega), \hat{q}_{m'\tau'}(\omega')] = (\pi\hbar/\Omega_r Z) \delta_{mm'} \delta_{\tau\tau'} \delta(\omega - \omega')$, where $\tau, \tau' = \{R, L\}$. We also introduce the ladder operator for the inductor charge via $\hat{Q}_L = \hat{q}_L + \hat{q}_L^\dagger$, where $[\hat{q}_L, \hat{q}_L^\dagger] = \hbar/2\omega_0 L$ and $\omega_0 = (LC)^{-1/2}$.

At $x = 0$, the quantum Maxwell-Bloch equations for our problem read

$$\nabla_x(\hat{Q}_{-R} + \hat{Q}_{-L})|_{x=0^-} = \nabla_x(\hat{Q}_{+R} + \hat{Q}_{+L})|_{x=0^+} \quad (4)$$

$$\frac{\nabla_x(\hat{Q}_{+R} + \hat{Q}_{+L})}{c}|_{x=0^+} = -\left(\frac{\hat{Q}_0}{C_c} + L\ddot{\hat{Q}}_L\right) \quad (5)$$

$$LC\ddot{\hat{Q}}_L - (\hat{Q}_0 - \hat{Q}_L) = Cg\hbar(\hat{S}_z \cot 2\xi + (\hat{S}^+ + \hat{S}^-)/2) \quad (6)$$

$$\hat{S}^- + [i(E/\hbar) + \Gamma_2]\hat{S}^- = ig(\hat{S}_z - \cot 2\xi \hat{S}^-)(\hat{Q}_0 - \hat{Q}_L) \quad (7)$$

$$\hat{S}_z + \Gamma_1(\hat{S}_z - S_z^0) = (ig/2)(\hat{S}^- - \hat{S}^+)(\hat{Q}_0 - \hat{Q}_L). \quad (8)$$

Here, we have introduced phenomenological longitudinal and transverse TLS relaxation rates, $\Gamma_1 = T_1^{-1}$ and $\Gamma_2 = T_2^{-1}$, and $S_z^0 = [\hat{Q}_{-R} + \hat{Q}_{-L} - \hat{Q}_{+R} - \hat{Q}_{+L}]|_{x=0}$. $S_z^0 = -(N/2) \tanh(E/2k_B T)$ is the equilibrium expectation value for \hat{S}_z when the TLSs are decoupled from the fields. Assuming we are in the low-temperature regime, i.e. $k_B T \ll E$, we take $S_z^0 \approx -N/2$. The first three equations above are quantum generalizations of the Kirchhoff voltage law, and the last two equations are quantum Bloch equations describing the coupling of the TLSs to the photon fields.

We now perform a series of standard approximations which maps the above equations to a form often seen in quantum optics literature describing an ensemble of two-level atoms in an optical cavity [20]. Since we have a high- Q resonator we perform the Markov approximation, where we replace $\sqrt{\omega}$ by $\sqrt{\omega_r}$ in the mode expansion Eq. (3) and extend the lower limit of the integral to negative infinity. We now go to a frame rotating at the pump frequency Ω , and use Greek letters to define operators in the rotating frame, i.e. $\hat{\theta}_{m\tau}(t) = \hat{q}_{m\tau}(t)e^{i\Omega t}$, $\hat{\theta}_L(t) = \hat{q}_L(t)e^{i\Omega t}$, $\hat{\Sigma}^\pm(t) = \hat{S}^\pm(t)e^{\mp i\Omega t}$, and $\hat{\Sigma}_z(t) = \hat{S}_z(t)$. Performing the slowly-varying envelope approximation on the $\hat{Q}_L(t)$ term and with the usual rotating-wave approximation, Eqs. (4)-(8) can then be rewritten as

$$(\partial_t - i\Omega)\hat{\theta}_1 = 0 \quad (9)$$

$$ZC_c(\partial_t - i\Omega)(\hat{\theta}_{+R} - \hat{\theta}_{+L}) = \hat{\theta}_0 - LC_c(\Omega^2 + 2i\Omega\partial_t)\hat{\theta}_L \quad (10)$$

$$-LC(\Omega^2 + 2i\Omega\partial_t)\hat{\theta}_L = \hat{\theta}_0 - \hat{\theta}_L + (Cg\hbar/2)\hat{\Sigma}^- \quad (11)$$

$$(\partial_t + i\Delta + \Gamma_2)\hat{\Sigma}^- = ig\hat{\Sigma}_z(\hat{\theta}_0 - \hat{\theta}_L) \quad (12)$$

$$2\partial_t\hat{\Sigma}_z + 2\Gamma_1(\hat{\Sigma}_z - \Sigma_z^0) = ig[\hat{\Sigma}^-(\hat{\theta}_0^\dagger - \hat{\theta}_L^\dagger) - h.c.], \quad (13)$$

where $\Delta = E/\hbar - \Omega$ is the TLS detuning, and $\hat{\theta}_{\{0,1\}} = \hat{\theta}_{-R} \pm \hat{\theta}_{-L} - \hat{\theta}_{+R} \mp \hat{\theta}_{+L}$. We note that the voltage fields propagating along the transmission lines relate to the charge fields $\hat{\theta}_{m\tau}$ through $\hat{v}_{m\tau}(t) = -c^{-1} \nabla_x \hat{\theta}_{m\tau}(x, t)|_{x=0}$.

We solve Eqs. (9)-(13) for $N \gg 1$ where the dynamics of the quantum system can be described semi-classically [24]. We treat each field $\phi(t)$ as a c -number and assume it has a steady-state mean part $\bar{\phi}$ and a fluctuating part $\delta\phi(t)$ which models the noise arising from the incident voltage on the transmission lines. Assuming small fluctuations, we linearize Eqs. (9)-(13) with respect to these fluctuations about the steady-state value.

The steady-state solution to the transmission amplitude $\bar{v}_{+R}/\bar{v}_{-R}$ is plotted in Fig. 2(a) for real \bar{v}_{-R} (input voltage am-

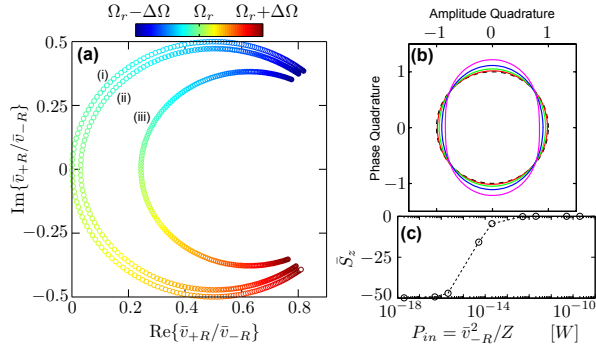


FIG. 2: (a) Steady-state solution for the transmission with $N = 100$, and (i) $\bar{v}_{-R} = 10\mu\text{V}$; (ii) $\bar{v}_{-R} = 1\mu\text{V}$; and (iii) $\bar{v}_{-R} = 0.05\mu\text{V}$. Here, $\Delta\Omega \approx 0.0003\omega_0$. (b) Noise ellipses for $\bar{v}_{-R} = 2\mu\text{V}$, $\Omega = \Omega_r$, and $N = 100$ (red), 300 (green), 600 (blue), and 1000 (magenta). The dashed line is quadrature-independent noise with no TLSs. (c) Plot of population imbalance, \bar{S}_z , as a function of input power for $N = 100$.

plitude) near the resonance frequency Ω_r . Blue points correspond to pump frequencies below Ω_r and red points to those above Ω_r . The solutions are plotted for three different values of \bar{v}_{-R} , and the parameters used are $C_c = 0.01\text{pF}$, $C = 0.3\text{pF}$, $Z = 50\Omega$, $f_0 = \omega_0/2\pi = 6\text{GHz}$, $T_1 = 300\text{ns}$, $T_2 = 30\text{ns}$, $d \approx 70\text{nm}$ and $N = 100$. We also assume the TLSs to be in resonance with the LC resonator and fix the TLS energy to $E = \Omega_r$ throughout and take $\Delta_A = \Delta_0$. We then find $\Omega_r \approx 0.9837\omega_0$. In Fig. 2(c), \bar{S}_z (TLS population imbalance) is plotted as a function of the input power, P_{in} . As P_{in} increases \bar{S}_z approaches zero signifying TLS saturation. We see that saturation occurs for $P_{in} \gtrsim 10^{-13}\text{W}$. Fig. 2(a) shows that the transmission deviates very little from the defect-free (no TLSs) limit for saturated TLSs. This is expected since only a small fraction of the total energy is stored in the TLSs when they are saturated.

We now move on to obtaining the noise in the transmitted voltage. Solving the linearized equations the transmitted charge fluctuations can be written in terms of the two input fluctuations as

$$\mathbf{A}_{+R}(\omega)\delta\Theta_{+R}(\omega) = \mathbf{A}_{-R}(\omega)\delta\Theta_{-R}(\omega) + \mathbf{A}_{+L}(\omega)\delta\Theta_{+L}(\omega), \quad (14)$$

where ω is the frequency deviation measured from the pump frequency Ω , $\delta\Theta_{m\tau}(\omega) = (\delta\theta_{m\tau}(\omega), \delta\theta_{m\tau}^*(-\omega))^T$, and the elements of the coefficient matrices $\mathbf{A}_{m\tau}(\omega)$ are given in the Supplementary Material. To study the quadrature-dependence of the noise in the transmitted voltage we introduce generalized voltage fluctuation variables $\delta v_{m\tau}(\omega, \varphi) = [e^{-i\varphi}\delta v_{m\tau}(\omega) + e^{i\varphi}\delta v_{m\tau}^*(-\omega)]/2$, where φ is the quadrature angle measured with respect to the real axis. We focus on the symmetrized correlator of these fluctuations, i.e. $S_{+R}(\omega, \omega', \varphi) = \langle \{\delta v_{+R}(\omega, \varphi), \delta v_{+R}^*(\omega', \varphi)\} \rangle$, where $\{A, B\} = AB + BA$. Assuming that the incoming fluctuations, $\delta v_{-R}(t)$ and $\delta v_{+L}(t)$, are characterized by a quadrature-independent white noise spectrum s_0 (for thermalized transmission lines it is $s_0^{\text{th}} =$

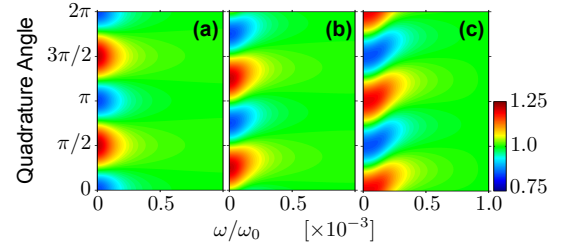


FIG. 3: Colour intensity plot of the normalized noise power $s_{+R}(\omega, \varphi)/s_0$ on the (ω, φ) -plane for pump frequencies on and away from resonance, $\bar{v}_{-R} = 2\mu\text{V}$ and $N = 1000$. Plots correspond to noise centred around (a) west; (b) northwest; and (c) north points, where north is defined as the top point on the resonance circle.

$2\pi\hbar Z\Omega_r \coth(\hbar\Omega_r/2k_B T)$), we have

$$\langle \{\delta v_{|-R,+L}(\omega, \varphi), \delta v_{|-R,+L}^*(\omega', \varphi)\} \rangle = s_0\delta(\omega - \omega'). \quad (15)$$

Using Eqs. (14) and (15) together with $\delta v_{+R}(\omega, \varphi) \approx -2iZ\Omega_r\delta\theta_{+R}(\omega, \varphi)$, $S_{+R}(\omega, \omega', \varphi) = s_{+R}(\omega, \varphi)\delta(\omega - \omega')$ can be straightforwardly obtained. (see Supplementary Material for details). In the following, we focus on the resulting spectral density of the noise, $s_{+R}(\omega, \varphi)$.

We first focus on the on-resonance case (where $\text{Im}\{\bar{v}_{+R}\} = 0$). Fig. 2(b) plots noise ellipses centred at this resonance point for $\bar{v}_{-R} = 2\mu\text{V}$ and various N . Here, we are plotting the $\omega = 0$ component of the noise spectral density normalized by s_0 . The noise ellipse is defined such that every vector from the origin to a point on the ellipse makes an angle φ (quadrature angle) with respect to the positive real axis and has length $s_{+R}(\omega = 0, \varphi)/s_0$. In the defect-free limit, the noise ellipse is circular with radius 1 (the dashed line), which shows that in the absence of non-linearity the transmitted noise remains quadrature-independent. In the presence of TLSs, we obtain *squeezing* where the noise along amplitude (phase) quadrature is reduced below (enhanced above) the noise of the incoming fluctuations. Eccentricity of the noise ellipse increases as the number of TLSs is increased.

Fig. 3 is a colour intensity plot of the normalized noise power $s_{+R}(\omega, \varphi)/s_0$ on the (ω, φ) -plane for on- and off-resonance pump frequencies. Here, $\bar{v}_{-R} = 2\mu\text{V}$ and $N = 1000$ are both fixed. We now use the convention where north corresponds to the point at the top of the resonance circle in Fig. 2(a), and west to the left-most point on the circle and so on. Then, the three plots correspond to the noise centred around (a) west; (b) northwest; and (c) north. The results show that the major axis of the noise ellipse is always along the phase direction. Our results are consistent with experiments, where fluctuations are also primarily observed in the direction tangent to the resonance circle [12].

In Fig. 4(a) we plot the normalized excess phase noise power, $s_{\text{exc}}^{\text{ph}}(\omega) := [s_{+R}(\omega, \varphi = \pi/2) - s_0]/s_0$ and negative of the normalized excess amplitude noise, $-s_{\text{exc}}^{\text{amp}}(\omega) := -[s_{+R}(\omega, \varphi = 0) - s_0]/s_0$, as a function of frequency deviation away from resonance, ω . Here we use $\bar{v}_{-R} = 2\mu\text{V}$ and

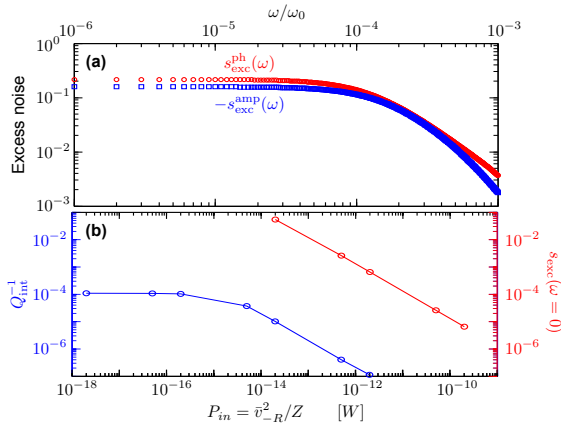


FIG. 4: (a) Frequency-dependence of the excess phase noise power and negative of the excess amplitude noise power for $\bar{v}_{-R} = 2\mu\text{V}$ and $N = 1000$. Roll-off at $\approx \omega/\omega_0 = 10^{-4}$ can be seen. (b) Normalized excess phase noise at $\omega = 0$ and inverse of the internal quality factor as a function of input power ($\Omega = \Omega_r$).

$N = 1000$. Both noises roll off at the resonator bandwidth $\omega_{\text{roll}}/\omega_0 \approx 10^{-4}$. From the steady-state solution the quality factor of the resonator is estimated to be $Q_r \approx 9800$, which is consistent with the plot. We see that the phase noise stays above the incoming noise s_0 while the amplitude noise remains below this value signifying squeezing. They both approach s_0 as the frequency deviates sufficiently beyond the resonator bandwidth (see also Fig. 3). For $\omega \gg \omega_{\text{roll}}$ we find $s_{\text{exc}}^{\text{ph}}(\omega) \sim (\omega/\omega_0)^{-2}$ and $-s_{\text{exc}}^{\text{amp}}(\omega) \sim (\omega/\omega_0)^{-2.9}$.

In Fig. 4(b) we plot the loss tangent, Q_{int}^{-1} for the pump frequency on resonance and $N = 100$. This was found numerically by fitting the transmission amplitude to a circuit model as a function of $[V(1 + Q_{\text{ext}}/Q_{\text{int}})]^2/Z \approx V^2/Z$. Here, V is the voltage across capacitor C (as shown in Fig. 1) and $Q_{\text{ext}} = 2(C + C_c)/(\omega_0 Z C_c^2)$ is the external quality factor. The above approximation holds because our resonator is over-coupled. At low amplitude the loss is constant, and at high amplitude the slope is ≈ -1 as the spins are saturated. This is in agreement with the semi-classical theory for a single TLS type. For the standard tunneling model distribution the density of defects follows $P(\Delta_A, \Delta_0) = P_0/\Delta_0$ and the superposition of the loss from different TLSs give a slope of $-1/2$ in the high power regime [3], as observed in amorphous films.

In the same figure the excess phase noise $s_{\text{exc}}(\omega = 0)$ is plotted. In the same high power regime as the loss tangent, the partially saturated TLSs exhibit phase noise with a slope of -1 , which disagrees with the power dependence observed in experiment [9]. This suggests that a correct description for the phase noise power dependence necessitates the inclusion of intrinsic stochastic fluctuations of the TLSs. Indeed, intrinsic TLS noise causes dielectric constant fluctuations and

can lead to observable noise [13]. We reiterate, however, that squeezing phenomenon itself is present regardless of deterministic or stochastic nature of TLS dynamics.

In conclusion, we have developed a theoretical framework applicable to circuits containing transmission lines, lumped circuit elements, and TLS defects, building upon previous work in quantum optics. It serves as a first step toward a quantitative theory for noise in these circuits. We found that quadrature-independent incident noise is generally squeezed once transmitted through a lumped circuit containing TLSs even when the latter evolve deterministically. Extensions of the model could allow for further quantitative results on noise due to TLSs, including the treatment of the standard tunneling model distribution of TLSs and incorporating intrinsic TLS fluctuations.

Acknowledgments: S. T. thanks Lev S. Bishop for discussions. S. T. and V. G. were supported by the Intelligence Advanced Research Projects Activity (IARPA) through the US Army Research Office award W911NF-09-1-0351.

-
- [1] W. A. Philipps, Rep. Prog. Phys. **50**, 1657 (1987).
 - [2] S. Hunklinger and W. Arnold, *Physical Acoustics*, edited by W. P. Mason and R. N. Thurston, (Academic, New York, 1976), Volume XII.
 - [3] M. v. Schickfus and S. Hunklinger, J. Phys. C **9**, L439 (1976); Physics Letters A **64**, 144 (1977).
 - [4] J. M. Martinis *et al.*, Phys. Rev. Lett. **95**, 210503 (2005).
 - [5] H. Wang *et al.*, Appl. Phys. Lett. **95**, 233508 (2009).
 - [6] H. Paik and K. D. Osborn, App. Phys. Lett. **96**, 072505 (2010).
 - [7] R. W. Simmonds *et al.*, Phys. Rev. Lett. **93**, 077003 (2004).
 - [8] A. Wallraff *et al.*, Nature **431**, 162 (2004); M. A. Sillanpää, J. I. Park, and R. W. Simmonds, *ibid.* **449**, 438 (2007).
 - [9] J. Gao, Ph.D. Thesis, California Institute of Technology (2008).
 - [10] J. Gao *et al.*, Appl. Phys. Lett. **92**, 152505 (2008); S. Kumar *et al.*, *ibid.* **92**, 123503 (2008).
 - [11] J. Gao *et al.*, arXiv:1008.0046v1.
 - [12] J. Gao *et al.*, App. Phys. Lett. **90**, 102507 (2007).
 - [13] J. Gao *et al.*, App. Phys. Lett. **92**, 212504 (2008).
 - [14] M. Constantin, C. C. Yu, and J. M. Martinis, Phys Rev. B **79**, 094520 (2009).
 - [15] B. Yurke *et al.*, Phys. Rev. Lett. **60**, 764 (1988).
 - [16] M. A. Castellanos-Beltran *et al.*, Nature Phys. **4**, 929 (2008).
 - [17] D. Rugar and P. Grütter, Phys. Rev. Lett. **67**, 699 (1991).
 - [18] J. Suh *et al.*, Nano Lett. **10**, 3990 (2010).
 - [19] R. E. Slusher *et al.*, Phys. Rev. Lett. **55**, 2409 (1985).
 - [20] L. A. Lugiato, in *Progress in Optics XXI*, edited by E. Wolf (North-Holland, Amsterdam, 1984).
 - [21] B. Yurke, Phys. Rev. A **29**, 408 (1984).
 - [22] B. Yurke and J. S. Denker, Phys. Rev. A **29**, 1419 (1984).
 - [23] G. Baier and M. v. Schickfus, Phys. Rev. B **38**, 9952 (1988); A. Holder and C. Musgrave, private communication.
 - [24] H. J. Carmichael, L. Tian, W. Ren, and P. Alsing, in *Cavity Quantum Electrodynamics*, ed. P. R. Berman, Academic Press, Boston, 1994, p. 381.